Open access • Journal Article • DOI:10.1515/CORRREV-2013-0023

A critical review of the influence of hydrogen on the mechanical properties of medium-strength steels — Source link

Qian Liu, Andrej Atrens

Institutions: University of Queensland

Published on: 01 Dec 2013 - Corrosion Reviews (De Gruyter)

Topics: Hydrogen embrittlement, Environmental stress fracture, Fatigue limit, Embrittlement and Ductility

DOI 10.1515/corrrev-2013-0023 — Corros Rev 2013; 31(3-6): 85–103

Qian Liu and Andrej Atrens*

A critical review of the influence of hydrogen on the mechanical properties of medium-strength steels

Abstract: As medium-strength steels are promising candidates for the hydrogen economy, it is important to understand their interaction with hydrogen. However, there are only a limited number of investigations on the behavior of medium-strength steels in hydrogen. The existing literature indicates that the influences of hydrogen on the tensile properties of medium-strength steels are mainly the following: (i) the steel can be hardened by hydrogen, as demonstrated by an increase in the yield stress or ultimate tensile stress; (ii) some steels can be embrittled by hydrogen, as revealed by lower yield stress or ultimate tensile stress; (iii) in most cases, these steels may experience hydrogen embrittlement (HE), as indicated by a reduction in ductility. The degree of HE mainly depends on the test conditions and the steel. The embrittlement can lead to catastrophic brittle fracture in service. The influence of hydrogen on the fatigue properties of medium-strength steels is dependent on many factors such as the stress ratio, temperature, yield stress of the steel, and test frequency. Generally, the hydrogen influence on fatigue limit is small, whereas hydrogen can accelerate the fatigue crack growth rate, leading to a shorter fatigue life. Inclusions are an important factor influencing the properties of medium-strength steels in the presence of hydrogen. However, it is not possible to predict the influence of hydrogen for any particular steel that has not been experimentally evaluated or to predict service performance. It is not known why similar steels can have different behavior, ranging from good resistance to significant embrittlement. A better understanding of the microstructural characteristics is needed.

Keywords: hydrogen embrittlement; mechanical properties; medium-strength steel.

***Corresponding author: Andrej Atrens,** Materials Engineering, The University of Queensland, St. Lucia, QLD 4072, Australia, e-mail: andrejs.atrens@uq.edu.au
Qian Liu: Materials Engineering, The University of Queensland, St. Lucia, QLD 4072, Australia

1 Introduction

In 1874, Johnson reported the degradation of mechanical properties of iron and steel due to hydrogen. He described the phenomenon as: 'This change is at once made evident to any one by the extraordinary decrease in toughness and breaking strain of the iron so treated, and is all the more remarkable as it is not permanent, but only temporary in character, for with lapse of time the metal slowly regains its original toughness and strength' (Johnson, 1874). Since then, there have been many investigations into the influence of hydrogen on the mechanical properties of steels. Comprehensive reviews from different viewpoints have been published (Barnoush, 2011; Ćwiek, 2010; Elboujdaini & Revie, 2009; Eliaz, Shachar, Tal, & Eliezer, 2002; Gangloff & Somerday, 2012; Hirth, 1980; Lynch, 2012; Nagumo, 2004; Oriani, Hirth, & Smialowski, 1985; Raja & Shoji, 2011). Generally, hydrogen degradation is classified into five types (Ćwiek, 2010; Lino, 1985): (i) cracking from precipitation of internal hydrogen, leading to shatter cracks, flakes, and fish-eye fractures; (ii) hydrogen attack; (iii) hydrogen blistering; (iv) cracking from hydride formation; and (v) hydrogen embrittlement (HE). Ćwiek (2010) has given a brief description of each damage type and some prevention methods. In this review, we mainly focus on the fifth type of hydrogen-induced damage – HE.

HE is the hydrogen-induced decrease in the properties of steel components such as reduced ductility and tensile strength, subcritical crack growth under monotonic loading, and increased fatigue crack growth (FCG) rates. Some standards for HE measurement are given in the following references (ASTM, 2011, 2012a,b).

HE can be divided into two types (Raja & Shoji, 2011): (i) 'internal hydrogen embrittlement' (IHE), which is due to the preexisting hydrogen already inside the steel, such as from pickling during manufacture, and (ii) 'hydrogen environment embrittlement', wherein hydrogen is from the environment, such as from corrosion in aqueous solutions, cathodic protection, and hydrogen gas. This latter case is the main focus of most research.

High-strength (and ultra-high-strength) martensitic steels with yield strengths higher than about 1400 MPa (hardness higher than 38 on the Rockwell C scale) are particularly susceptible to IHE (Raja & Shoji, 2011; Ramamurthy & Atrens, 2013), even when the hydrogen content is <1 ppm (Ramamurthy & Atrens, 2013). Although laboratory vessels can be made out of exotic materials, there is an economic incentive to use less expensive materials such as steels, as the technology is scaled up. Thus, there is a requirement to understand the interaction of hydrogen with medium-strength steels that may be suitable for hydrogen service.

This review focuses on the influence of hydrogen on the properties of medium-strength steels, typically with tensile strengths in the range of 600–1000 MPa.

2 Entry of hydrogen

Perng and Wu (2003) reviewed the mechanisms of hydrogen entry into metals. For steels in service, there are two sources of hydrogen from the environment: (i) hydrogen gas and (ii) corrosion. The overall gas-solid interaction is defined in terms of three steps: physisorption, chemisorption, and absorption. Physisorption is reversible, and the energy for adsorption is low, usually <20 kJ mol^{-1} (Pasco, 1985). It is much easier for physisorption to achieve equilibrium at room temperature. At much higher temperatures, chemisorption is the main way for hydrogen uptake. The energy for adsorption is related to the bond energies of an M-H and H-H pair. For a Fe-H bond, the energy is 282 kJ mol^{-1} (Pasco, 1985), which is much higher than physisorption. Usually, the physisorbed hydrogen transfers into chemisorbed hydrogen before entering into the metal.

Corrosion, the other main hydrogen source, can involve hydrogen in the cathodic partial reaction. The hydrogen evolution reaction (HER) may proceed through the following steps (Lasia & Gregoire, 1995; Zakroczymski, 1985):

(i) $H_3O^+ + M + e \rightarrow M{\cdot}H_{ads} + H_2O$ (in acid solutions) (1)

or $H_2O + M + e \rightarrow M{\cdot}H_{ads} + OH^-$ (in alkaline solutions) (2)

(ii) $2M{\cdot}H_{ads} \rightarrow H_2 + 2M$ (chemical desorption) (3)

or $M{\cdot}H_{ads} + H_3O^+ + e \rightarrow H_2 + H_2O + M$ (in acid solutions) (4)

or $M{\cdot}H_{ads} + H_2O + e \rightarrow H_2 + OH^- + M$ (in alkaline solutions) (5)

$M{\cdot}H_{ads}$ represents a hydrogen atom adsorbed on the metal surface. Molecular hydrogen gas can be formed and then can desorb from the sample surface, through Eqs. (3) to (5), or hydrogen can enter into the metal through the hydrogen absorption reaction (HAR). Two models of hydrogen entry were proposed, respectively, by Bockris, McBreen, and Nanis (1965) (Model A) and Bagotskaya et al. (Model B) (Zakroczymski, 1985). For Model A, the adsorbed state is an intermediate stage through which electrolytic hydrogen enters into the metal substrate. It is identical to that which leads to hydrogen evolution. The reaction sequence at the cathode surface is as follows (in acid):

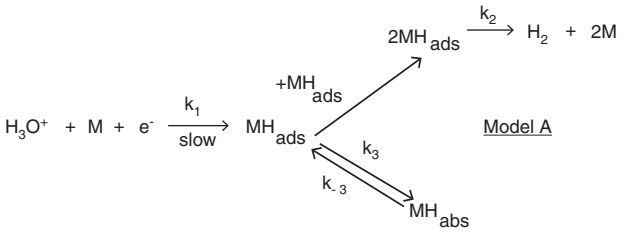

(6)

$M{\cdot}H_{abs}$ refers to the absorbed hydrogen inside the metal. The permeation rate should be proportional to the coverage of the metal surface by adsorbed hydrogen atoms, θ_H.

For Model B, HAR and HER do not occur dependently. The intermediate states for hydrogen entering the metal lattice and hydrogen evolution are different. The following schematic gives the reaction sequence at the cathode surface.

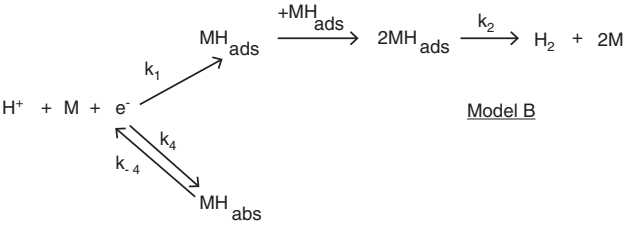

(7)

Bockris et al. (1965) studied HER on pure iron in 0.1 N H_2SO_4 and 0.1 N NaOH. Their results showed a coupled discharge chemical desorption mechanism for hydrogen evolution on iron at low overpotentials (more negative than -1.02 V_{NHE}). The adsorption of hydrogen on the metal surface followed Langmuir adsorption, implying that hydrogen was absorbed *via* Model A.

The processes mentioned above do not involve the presence of an oxide film, which makes the hydrogen absorption more complicated, for example, the film can reduce the apparent hydrogen diffusivity (Perujo, Serra, Alberici, Tominetti, & Camposilvan, 1997).

3 Equivalence of gaseous and electrolytic charging

Two methods have been used to simulate metals used in hydrogen environments: (i) electrochemical charging

(Glowacka & Swiatnicki, 2003; Glowacka, Wozniak, & Swiatnicki, 2005; Herms, Olive, & Puiggali, 1999; Li, Gangloff, & Scully, 2004; Pan et al. 2002; Panagopoulos, El-Amoush, & Georgarakis, 2005; Wang, 2009; Wang, Akiyama, & Tsuzaki, 2005a) for which the specimen is placed in an electrochemical cell, and either a current density i_c or a negative potential, E_c, is applied to the specimen for charging, and (ii) gas-phase hydrogen charging (Hardie, Xu, Charles, & Wei, 2004; West & Louthan, 1982), typically at an elevated temperature. Theoretically, the same amount of hydrogen can be charged into a metal through the different charging methods, if appropriate charging parameters are chosen. The gaseous charging and electrolytic charging are equivalent.

The hydrogen concentration in equilibrium is given by Sievert's law. However, the f/P data (f is the fugacity, P is pressure) for hydrogen given by Holley, Worlton, and Zeigler (1958) indicated that it was more reasonable to use fugacity f_{H_2} rather than pressure P_{H_2} in Sievert's law. Therefore, in a hydrogen gas environment, the hydrogen concentration, C_H, in equilibrium dissolved in a solid metal is proportional to the square root of hydrogen fugacity, given by

$$C_H = S\sqrt{f_{H_2}}, \tag{8}$$

where S is a solubility constant and f_{H_2} is the hydrogen fugacity.

Bockris and Subramanyan (1971) investigated the equivalent pressure of molecular hydrogen in metals in terms of overpotential, η, during HER, where η is the deviation of the applied potential, E_c, from the equilibrium potential of HER at unit fugacity, E_H^0. In acid solutions, it is generally thought that HER is controlled by the fast discharge-slow electrochemical desorption sequence (Atrens, Mezzanotte, Fiore, & Genshaw, 1980). In this case, the relationship between f_{H_2} and the electrolytic charging conditions as specified by E_c is given by

$$f_{H_2} = \exp\left(-\frac{2\eta F}{RT}\right) = \exp\left(-\frac{2(E_c - E_H^0)F}{RT}\right). \tag{9}$$

Meanwhile, in a permeability experiment, the hydrogen concentration on the entry side is proportional to the current density at steady state and given by (Hadam & Zakroczymski, 2009)

$$C_H = \frac{i_\infty^e L}{FD}, \tag{10}$$

where i_∞^e is the steady current density at a given negative potential, L is the sample thickness, F is Faraday constant, and D is the hydrogen diffusion coefficient. Under the sole assumption that Sievert's law applies to both gas-phase permeation studies and electrolytic charging studies, then

$$i_\infty^e = \frac{FDS}{L}(f_{H_2}^e)^{1/2} = \frac{FDS}{L}\exp\left(-\frac{(E_c - E_H^0)F}{RT}\right) \tag{11}$$

$$i_\infty^g = \frac{FDS}{L}(f_{H_2}^g)^{1/2} \tag{12}$$

Eq. (11) indicates that the plot of ln i_∞ and E_c should be linear, which was verified by the results in the study of Atrens et al. (1980). Thus, it is possible to conduct equivalent electrolytic and gaseous permeability studies by the choice of an appropriate applied potential E_c.

Compared with gas-phase hydrogen charging, the electrochemical charging method is easier to operate. With the help of an established relationship between the gas-phase hydrogen charging and the electrochemical charging, proper potential could be set during electrochemical charging to provide a better stimulation of the actual H condition in service. In this case, the results from mechanical or fatigue tests with hydrogen charging would be more reliable for predicting the safe life of the steel. This could help the designer choose the proper steels for their designs.

4 Hydrogen permeation

To better understand the influence of hydrogen on steels and to estimate the safe life more accurately, it is important to know the hydrogen diffusion coefficient, D, and the hydrogen concentration, C_H, in steels. It is then possible to assess how much hydrogen is in the steel and how far the hydrogen can diffuse in a given period in service.

The permeability method is the most common method used to measure these two parameters. This method is based on a membrane using either gas-phase charging or electrochemical charging. Gas-phase charging usually is applied at elevated temperatures, typically above 150 C. Electrochemical charging is more commonly used at temperatures up to 100 C. Hydrogen absorption, permeation, and desorption can be measured using the electrochemical double cell, which was first described by Devanathan and Stachurski (1962). Hydrogen atoms are generated on one side of the membrane (the entry side) and the diffusing hydrogen atoms are oxidized on the other side (the exit side). On the entry side, solutions used are usually NaOH or H_2SO_4 aqueous solution; on the exit side, the solution is typically NaOH aqueous solution (Addach,

Berçot, Rezrazi, & Takadoum, 2009; Atrens et al., 1980; Beck, Bockris, Genshaw, & Subramanyan, 1971; Frappart et al., 2012; Grabke & Riecke, 2000; Hashimoto & Latanision, 1988a; Tau, Chan, & Shin, 1996; Yan & Weng, 2006; Zhang & Zheng, 1998). Figure 1 shows a typical cell used for permeability test (Atrens et al., 1980).

In the permeability method, the hydrogen in the metal is the sum of the reversible trapped hydrogen and the lattice hydrogen. Usually, the constant concentration model (Zhang, Zheng, & Wu, 1999) is proposed to evaluate the hydrogen diffusivity from the permeation tests. The boundary conditions are as follows:

$$t=0, C=0; \text{and} \, t>0, \begin{cases} C_{x=0}=C_0 \\ C_{x=L}=0 \end{cases}, \tag{13}$$

where t is the time, $C_{x=0}$ and $C_{x=L}$ are the hydrogen concentrations on the entry and exit surfaces, and C_0 is the uniform concentration that is determined by the input hydrogen fugacity or the applied potential. Based on these boundary conditions, the detailed calculation methods are described as follows:

(i) A common way for calculating D is the time lag method, which was proposed by Daynes (1920), derived from Fick's second law. The formula is

$$D=\frac{L^2}{6t_L}, \tag{14}$$

where L is the thickness of sample, t_L is the lag time; usually t_L is the time when $i \approx 0.63 i_\infty$. This method is simple because it does not take the absorption and desorption of hydrogen into consideration. However, the D obtained from this method is inversely proportional to the sample thickness, which is theoretically incorrect. A method similar to the time lag method is the half time method, $t_{1/2}$. $t_{1/2}$ is the time required for the permeation flux to attain a height half of the steady-state level (McBreen, Nonis, & Beck, 1966).

(ii) In the method of successive transients (Atrens et al., 1980), the subsequent rise or decay of the permeation current, i, is recorded after steady-state conditions have been achieved in the prior transient. A generalized transient can be defined in terms of a normalized current parameter, $\frac{i_\tau - i_\infty^0}{i_\infty^1 - i_\infty^0}$, and a dimensionless time parameter, $\tau=\frac{Dt}{L^2}$. This displacement of typical time and log τ axis provides a direct indication of D because

$$\log\tau=\log B+\log t, \tag{15}$$

where $B=DL^2$ is the displacement distance. Alternatively, once the experimental and master plots are brought into coincidence, each value of t fixes a value of τ, so that D may be calculated from

$$D=L^2 \log^{-1}\left(\log\frac{\tau}{t}\right). \tag{16}$$

(iii) A new model for hydrogen permeation proposed by Wang (1936) was simplified by Zhang and Zheng (1998), considering the absorption and desorption processes as a forward and a reverse jump. In this theory, the permeation process was considered as a one-dimensional process.

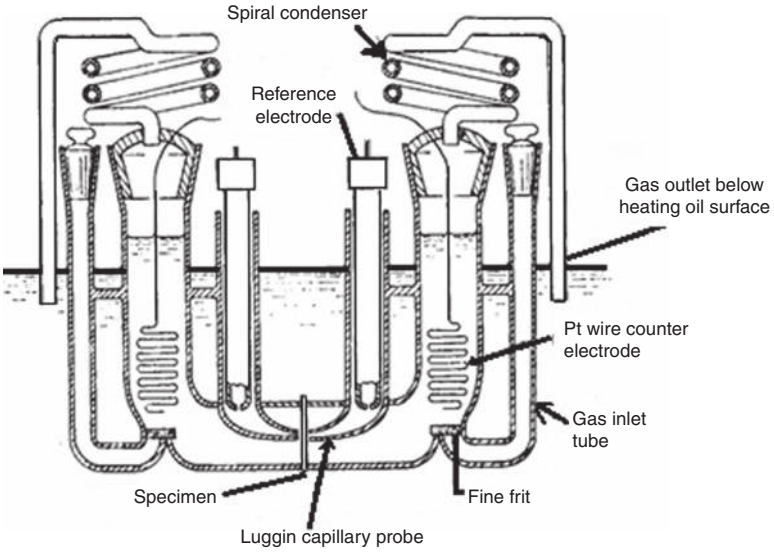

Figure 1 Schematic of an electrolytic permeability cell.
Reprinted from Atrens et al. (1980), with permission from Elsevier.

The diffusivity, D, is evaluated from fitting the measured-normalized permeation flux with the following equation:

$$\frac{J}{J_\infty}=1+2(2D+kL)\sum_{m=1}^{\infty}\frac{e^{-D\lambda_m^2 t}[k\cos(\lambda_m k)-D\lambda_m\sin(\lambda_m L)]}{[(D^2\lambda_m^2+k)L+2kD]}, \quad (17)$$

where J and J_∞ are the permeation flux at the time t and at the steady state, k is the desorption rate parameter, L is the sample thickness, and λ_m is the mth positive root of

$$\tan(\lambda_m L)=\frac{2kD\lambda_m}{D^2\lambda_m^2-k^2}. \quad (18)$$

The diffusivity, evaluated from the proposed model, for hydrogen diffusion in fully annealed commercially pure iron at room temperature was about 4×10^{-5} cm^2 s^{-1} (Zhang & Zheng, 1998), which was independent of sample thickness.

The diffusivity, D, can also be calculated by the following method from the shape of the hydrogen distribution. After measuring the hydrogen content distributions in specimens, using the least-square method based on Eq. (19) (Kanezaki, Narazaki, Mine, Matsuoka, & Murakami, 2008), D can be obtained.

$$C(x,t)=(C_s-C_u)\left\{1-\mathrm{erf}\left(\frac{x}{2\sqrt{Dt}}\right)\right\}+C_u \quad (19)$$

where x is the depth from the surface, t is the time of hydrogen charging, C_s is the saturated hydrogen content by the hydrogen charging, C_u is the hydrogen content of the uncharged specimen, and D is the temperature-dependent diffusion coefficient of hydrogen.

With knowing D, the hydrogen concentration in the steel can be calculated according to Eq. (10) (Hadam & Zakroczymski, 2009). Then, the evaluation of hydrogen influence on the properties of steels can be more reasonable.

5 HE mechanisms

A short summary is presented of HE mechanisms. These are mainly based on pressure, decohesion, surface adsorption, and enhanced plastic flow (Beachem, 1972; Birnbaum & Sofronis, 1994; Lynch, 2009; Mukhopadhyay, Sridhar, Parida, Tarafder, & Ranganath, 1999; Nelson, 1983; Petch & Stables, 1952; Popov & Nechai, 1967; Toribio, 1996; Troiano, 1960; Zapffe & Sims, 1941). Lynch (2012) has recently given an extensive review on the possible mechanisms for HE.

The pressure theory of hydrogen damage (Zapffe & Sims, 1941) attributes HE to the accumulation of hydrogen at voids or other internal surfaces, where hydrogen combines to form molecular hydrogen. A high internal pressure is created at these microstructural discontinuities that enhances void growth or initiates cracking. The hydrogen-enhanced decohesion (HEDE) mechanism (Mukhopadhyay et al., 1999; Toribio, 1996; Troiano, 1960) proposes that the atomic bonding of the sharp crack tip, or the particle-matrix interfaces ahead of cracks, or several tens of nanometers ahead of cracks where the tensile stress is maximum, or the position of maximum hydrostatic stress, is degraded in the presence of dissolved hydrogen. A lower stress is needed to initiate or propagate a crack. The surface adsorption theory (Petch & Stables, 1952) suggests that the surface free energy is decreased by hydrogen adsorption, and thus the fracture stress needed for a new surface is decreased. Hydrogen-enhanced local plasticity (HELP) (Birnbaum & Sofronis, 1994) is characteristic of atomic hydrogen that enhances the mobility of dislocations, causing locally reduced shear strength. This fracture process results in cracking by microvoid coalescence (MVC) along preferred crystallographic glide planes. HELP is a highly localized plastic failure process that causes macroscopic embrittlement. The adsorption-induced dislocation emission (AIDE) mechanism proposes (Lynch, 1988, 2009) that hydrogen adsorbed on the surface, and among the first few atomic layers, facilitates the nucleation of dislocations from the crack tip by weakening the interatomic bonds. In many cases, studies propose that these mechanisms are mixed (Birnbaum, 1989; Gangloff, 2003). These mechanisms of cracking may occur simultaneously, depending on the material and the environment variables.

6 Hydrogen influence on tensile properties

Understanding the influence of hydrogen on the tensile properties is important to the assessment of service performance. The tensile test accompanied with microscopy is often used to study the influence of hydrogen on mechanical properties, in which a specimen is loaded in uniaxial tension until failure. The specimen can be a smooth bar, a notched bar, or a plane strain specimen. The tensile test allows the measurement of the yield strength, ultimate strength, total elongation, and the reduction in cross-sectional area. Two approaches have been developed: (i) the slow strain rate test (Wang et al., 2005a; Wang,

2009; Wang, Akiyama, & Tsuzaki, 2007; Zakroczymski, Glowacka, & Swiatnicki, 2005), which increases strain until fracture, and (ii) the linearly increasing stress test (LIST) (Atrens, Brosnan, Ramamurthy, Oehlert, & Smith, 1993; Gamboa & Atrens, 2003a,b, 2005; Liu, Irwanto, & Atrens, 2013; Ramamurthy & Atrens, 2010; Ramamurthy, Lau, & Atrens, 2011; Villalba & Atrens, 2007, 2008a,b, 2009), which increases stress until fracture.

6.1 Ductility

Ductility is an important property of materials. The ductility can be quantified by (Dieter, 1961) (i) the fracture strain, ε_f%, which is the engineering strain at which a test specimen fractures during a uniaxial tensile test, or (ii) by the reduction of area at fracture, R_A%, which can be evaluated by the following equation:

$$R_A\% = \frac{A_i - A_f}{A_i} \times 100\%, \quad (20)$$

where A_i and A_f are the initial and the final fracture areas, respectively. It is reasonable to assess (i) the influence of hydrogen on ductility and ii) the significance of HE by the difference in values of fracture strain or R_A% obtained with or without hydrogen charging.

Tests by Marchetti, Herms, Laghoutaris, and Chêne (2011) showed that for the ferritic-martensitic steel T91, the elongation and the reduction of area decreased due to hydrogen charging. This is consistent with the influence of hydrogen on the ductility of A-106 steel (Sudarshan, Louthan, & McNitt, 1978). The ferritic-martensitic steel T91 could experience significant HE with hydrogen charging. Maier, Popp, and Kaesche (1995) showed that for 90MnV8, hydrogen charging caused a more significant reduction in ductility as the charging current density increased, as is shown by Figure 2A. In air, the effect of strain rate on elongation to fracture was only minor; Figure 2B shows that the ductility decreased at lower strain rates for specimens being hydrogen charged.

A trend of decreasing tensile ductility with increasing gas pressure was observed by Nanninga et al. (2012). The ductility of X52, X65, and X100 was significantly degraded by gaseous hydrogen. For example, compared with 76% in air, the R_A% of X100 reduced to 23% in hydrogen gas with a pressure of 27.6 MPa. The results presented by Arafin and Szpunar (2011) showed similar results for X80 and X100, indicating that both steels were highly vulnerable to HE at cathodic potentials, especially at a more negative potential. This agrees with the investigation of X80 by Moro et al. (2010). Torres-Islas, Salinas-Bravo, Albarran, and Gonzalez-Rodriguez (2005) found that the influence of hydrogen was considerable on the quenched, and both quenched and tempered X70, specimens. Sojka et al. (2011) found that the elongation reduced with hydrogen content in TRIP 800 steels, indicating that the steels were embrittled to different degrees depending on the hydrogen content in steels. Significant HE can be provoked for very high hydrogen content. Moon, Balasubramaniam, and Panda (2010) showed that rail steels of C-Mn, Cu-Mo, and Cr-Cu-Ni were susceptible to HE based on the reduction in both the elongation and R_A%.

Using LIST (Atrens et al., 1993; Gamboa & Atrens, 2003a,b, 2005; Liu et al., 2013; Oehlert & Atrens, 1996; Ramamurthy & Atrens, 2010; Ramamurthy et al., 2011; Villalba & Atrens, 2007, 2008a,b, 2009), Villalba and Atrens (2007) showed that hydrogen caused significant loss of ductility for some medium-strength steels (1019, MRB500, X1340F, YK5155S, 4145V, 10M40, X11M47, and HSAC840) in the form of smaller strain to fracture, ε_f%. For example, for the X1340F steel, ε_f% equaled 24% and 9% in air and in the sulfate pH ~2.1 solution used to charge hydrogen. The lower value of ε_f% obtained in solution

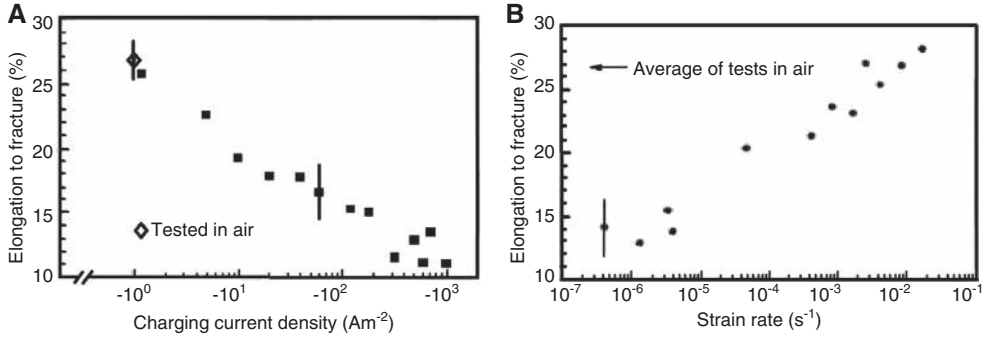

Figure 2 Elongation to fracture as a function of (A) charging current density, i_c, (($\dot{\varepsilon}$=1.4×10^{-6} s^{-1})) and (B) strain rate (i_c=-500 A m^{-2}), compared with a test run in air, T=293 K.
Reprinted from Maier et al. (1995) with permission from Elsevier.

implied that the steel had experienced some embrittlement, although the fracture surface did not show SCC features. In contrast, 1003 showed little ductility in the pH ~2.1 solution and brittle SCC features (Villalba & Atrens, 2007). The quenched and tempered 3.5NiCrMoV steel (Liu et al., 2013) also experienced some ductility reduction by smaller R_A% under hydrogen charging, which decreased more with decreasing applied potential (more hydrogen). This is essentially the same phenomenon as that showed in Figure 1A (Maier et al., 1995). However, it was notable that although the tested 3.5NiCrMoV steel slightly suffered from some HE, there was no SCC feature on the fracture surface, which was mostly covered by dimples. The appearance of HE only occurred after the onset of necking.

After hydrogen charging, the R_A% of 4307 and 1022QT reduced from 55% to 46% and from 52% to 43%, respectively (Lukito & Szklarska-Smialowska, 1997). Lukito and Szklarska-Smialowska (1997) defined a '% ductile mode' to represent the fraction of the neck that fractured by a ductile failure mode. The results showed that the variation in this parameter between the charged and the uncharged samples was very small for both steels. The decreases in '% ductile mode' after hydrogen charging were 1.3% and 1% for 4037 and 1022QT, respectively. This implied that hydrogen did not have a significant influence on the ductility of those two steels, indicating these two steels have good resistance to HE.

In conclusion, the ductility of materials can be influenced by hydrogen, but it is not always considerable. For some medium-strength steels, the reduction in ductility due to hydrogen was obvious, indicating that the steels have experienced HE, and would be expected to undergo unexpected brittle fracture if exposed in service under conditions producing hydrogen. However, there were some steels that showed good ductility with only a slight decrease in R_A% under hydrogen charging; these steels present good resistance to HE. There were similar steels with similar composition and microstructural characteristics that showed very different influence of hydrogen, ranging from good resistance to significant embrittlement (Gamboa & Atrens, 2003a,b, 2005; Villalba & Atrens, 2007, 2008a,b, 2009). Clearly, a better understanding of the interaction of hydrogen with microstructural characteristics is needed.

6.2 Embrittlement and hardening by hydrogen

Both HELP and AIDE mechanisms indicate that hydrogen could embrittle the steel, and the observations of enhanced dislocation nucleation and increased dislocation velocities in the presence of hydrogen and much research (Araújo et al., 2011; Cracknell & Petch, 1955; Hirth, 1980; Sudarshan et al., 1978) have verified this conclusion. Araújo et al. (2011) found that the API 5L X60 steel presented a softening process with hydrogen charging, observed by the decrease in yield strength and increase in the ductility. Sudarshan et al. (1978) showed that the yield point of A-106 steel was reduced by exposure to gaseous hydrogen, as did the fracture strength. Lukito and Szklarska-Smialowska (1997) presented that the tensile strengths of 4037 and 1022QT were slightly lower after being charged by hydrogen, indicating that hydrogen did not produce a significant effect on the tensile properties of these steels.

In contrast, there are many reports as well showing that hydrogen strengthened the materials. The slope of the stress-stain curve and the ultimate tensile strength (UTS) for the spheroidized low-alloy steel 90MnV8 (Maier et al., 1995) was not affected by hydrogen charging. Villalba and Atrens (2008b) found that X70 showed similar values of the UTS in air and with hydrogen charging, whereas the values of UTS of 4140H were higher with hydrogen charging. The investigation of three pipeline steels by Nanninga et al. (2012) showed that there were slight increases in yield and tensile strength by hydrogen. Nanninga et al. stated that gaseous hydrogen did not have a significant effect on either the yield or tensile strength. LIST research on 3.5NiCrMoV steel (Liu et al., 2013) also showed that the yield stress and the fracture stress were increasing slightly instead of decreasing with negatively increasing charging potential. A similar trend was observed for the ferritic-martensitic steel T91 (Marchetti et al., 2011). Based on the results from Villalba and Atrens (2007, 2008b), Marchetti et al. (2011), and Liu et al. (2013), it is concluded that for these steels, instead of degradation, hydrogen raised the yield stress and the fracture stress slightly; these materials were hardened by hydrogen. This phenomenon was reported by others as well (Abraham & Altstetter, 1995; Caskey, 1981; Louthan, Caskey, Donovan, & Rawl, 1972; Matsui, Kimura, & Moriya, 1979; Oguri, Takaki, & Kimura, 1982; Oriani & Josephic, 1980; Siddiqui & Abdullah, 2005; Thomson, 1978; West & Louthan, 1982). It was proposed that the hardening of materials with hydrogen could be interpreted as a result of hydrogen-dislocation interactions (Abraham & Altstetter, 1995; Louthan et al., 1972; Matsui et al., 1979; Oriani & Josephic, 1980). The increase in yield stress in the presence of hydrogen was explained by the inhibition of moving dislocation or impeding cross slip by hydrogen (Abraham & Altstetter, 1995; Oriani & Josephic, 1980).

It is concluded that hydrogen embrittles some medium-strength steels by giving lower yield stress or tensile stress. In some cases, the material was hardened in the presence of hydrogen presenting a higher yield stress or fracture stress. There were some other medium-strength steels, even though the reduction in ductility due to hydrogen was significant, hydrogen did not produce a significant influence on the UTS and yield stress, even under severe hydrogen charging conditions.

6.3 Fracture with hydrogen charging

The fracture surfaces obtained under hydrogen charging may be a mixture of topographies, as shown in Figure 3 (Gamboa & Atrens, 2003a), such as secondary cracks, corrugated irregular surface (CIS), tearing topography surface (TTS) (Toribio, Lancha, & Elices, 1991a), quasi-MVC (qMVC), MVC, and fast fracture surface (FFS) instead of pure MVC as often occurs on uncharged specimens. TTS, having spacing that is only slightly coarser than that of pearlite's, is characterized by a ridge pattern free from the pearlite microstructure. It occurred close to the free surface due to HE (Toribio, Lancha, & Elices, 1991b). CIS was characterized as porous irregular corrugated surfaces joined by rough slopes. It was described as a network of corrugated surfaces, displaying a network of branched channels joined by rough slopes. qMVC surface contained much flatter microvoids, similar to the MVC in pure ductile failure samples. This was attributed to some hydrogen entering the material but not in sufficient concentration to cause the morphology to resemble that of CIS. It is almost a ductile fracture. The MVC displayed dimples. FFS consisted of flat areas marked by tear lines. The orientation of the maples leaves in the FFS tended to far away from the crack initiation site, which was due to the crack propagating quickly away from the subcritical growth area.

Figure 4 presents the daisy-like features observed on the hydrogen-charged 3.5NiCrMoV specimens (Liu et al., 2013). The examination of the daisy-like features indicated

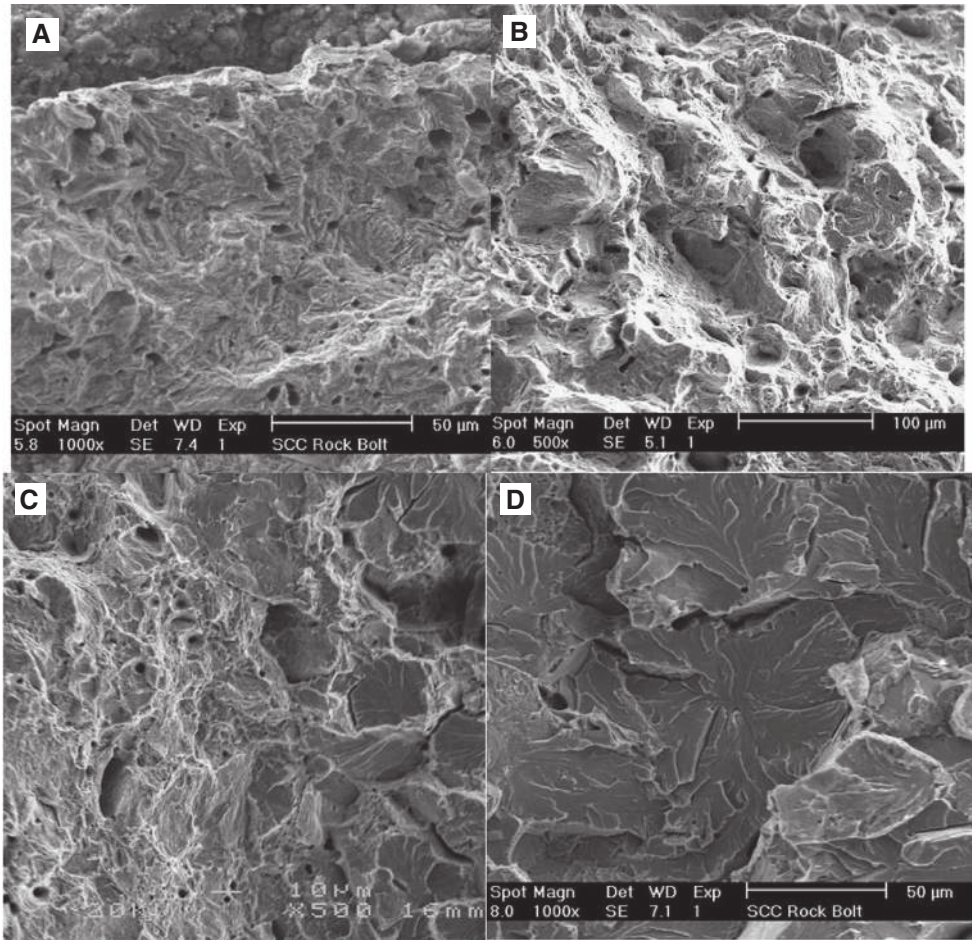

Figure 3 Typical features on a brittle surface: (A) TTS, (B) CIS, (C) qMVC-FFS, (D) FFS.
Reprinted from Gamboa and Atrens (2003) with permission from Elsevier.

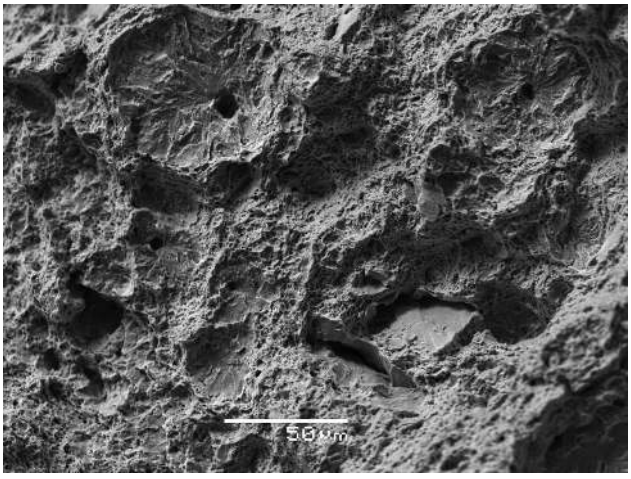

Figure 4 A view of the daisy-like round flat regions on the fracture surface of 3.5NiCrMoV steel tested in 0.1 M Na_2SO_4, pH=2 at -950 $mV_{Ag/AgCl}$.
Reprinted from Liu et al. (2013) with permission from Elsevier.

that there were inclusions in the centers of these features, implying these inclusions were probably the initiation sites of the hydrogen-related fracture events associated with the daisy-like features. Inclusions are an inevitable part of the microstructure of commercial steels such as 3.5NiCrMoV (Lynch, 1988; Popov & Nechai, 1967). Presumably, the hydrogen-inclusions interactions might lead to the occurrence of daisy-like features.

In some cases, there is no necking and only brittle fracture in the presence of hydrogen. However, necking may exist even in the presence of hydrogen, and the fractography can be dominated by ductile dimples. The investigations (Villalba & Atrens, 2007, 2008a,b, 2009) on X70 and 4145H showed that all the samples of X70 and 4145H showed ductile characteristics in all tested conditions, no matter, at the free corrosion potential, or at increasingly negative applied potential values up to -1500 mV. With decreasing applied potential, the aggressiveness of the environment increased on account of increasing hydrogen liberated the specimen surface. However, the fractography of X70 observed by Wang (2009) indicated that the average size of dimples after hydrogen charging was smaller than that of uncharged specimens and became smaller as the charging current density increased. The decrease in diameter of dimples reflected the loss of ductility of the steel. Moreover, Wang indicated that the fracture morphology can be influenced by the hydrogen charging process. The fracture surfaces, either hydrogen pre-charged or without hydrogen charging, were characterized by dimples, whereas under dynamic hydrogen charging, the fracture surface was dominated by the cleavage morphology. The different fracture surfaces obtained from pre-charged and dynamic charged specimens revealed that they were related to different fracture mechanisms. According to the experimental fracture morphology, HELP was responsible for the reduction of the fracture toughness in the former, with dimples all over the surface and HEDE for the latter, with the appearance of cleavage facets. This indicates that there can be different consequences with different hydrogen charging processes.

The influence of hydrogen on the fracture was presented by surface cracks as well, as shown in Figure 5 (Liu et al., 2013). Marchetti et al. (2011) stated that with hydrogen charging, (i) cracking occurred in the necked part and

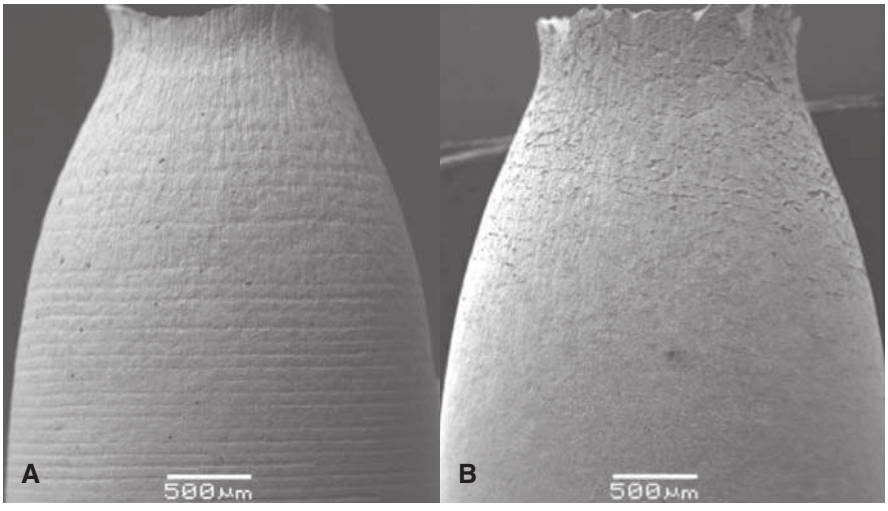

Figure 5 Overview of the necked part of the 3.5NiCrMoV steel tested (A) in air, no cracks observed, and (B) in 0.1 M Na_2SO_4, pH=2 at -950 $mV_{Ag/AgCl}$, cracks in the necked part.
Reprinted from Liu et al. (2013) with permission from Elsevier.

(ii) only occurred after the onset of necking and the brittle zone located at the edge of the fracture surface increased with charging current. Marchetti et al. (2011) proposed that (i) there was a critical hydrogen concentration for crack initiation and (ii) the extent of cracking directly depended on the hydrogen concentration. Meanwhile, Brass and Chêne (2006) found that there was a strong influence of the deformation mechanisms associated with the material microstructure on the strain-induced changes of the permeation current density. Thus, Marchetti et al. (2011) attributed the increase of apparent hydrogen diffusion coefficient (D_{app}), with increasing charging current, to the combination of the increased trapping rate on preexisting and strain-induced traps during the deformation and to H dragging by moving traps such as dislocations (Hashimoto & Latanision, 1988b). The consequence of increased D_{app} would be increased local hydrogen concentration and increased crack depth on the fracture surface.

In summary, due to hydrogen, brittle features such as CIS, TTS, qMVC, FFS, and daisy-like feature can be observed on the fracture surface. However, for steels having a good resistance to HE, the fracture surface was mainly occupied by dimples interpreted with small brittle features.

7 The hydrogen influence on fatigue

Fatigue occurs when a material is subjected to repeat loading and unloading. If the loads are above a threshold, microscopic cracks begin to form at the surface. Eventually, a critical size of the crack is reached, leading to sudden fracture. In the presence of hydrogen, in most cases, the fatigue properties are degraded.

7.1 Fatigue life and fatigue limit

Generally, fatigue life could be reduced drastically, for example, by more than 80%, in the presence of hydrogen (Balitskii, Krohmalny, & Ripey, 2000; Ćwiek, 2007; Fukuyama, Yokoyawa, Kudo, & Araki, 1985; Kuromoto, Guimarães, & Lepienski, 2004; Labidi, Habashi, Tvrdy, & Galland, 1992; Nagumo, Shimura, Chaya, Hayashi, & Ochiai, 2003; Tsuchida, Watanabe, Kato, & Seto, 2010), whereas the fatigue limit is lower but not much compared with no hydrogen charging (Capelle, Gilgert, & Pluvinage, 2010; Fukuyama et al., 1985; Kishi & Takano, 2010; Macadre, Yano, Matsuoka, & Furtado, 2011; Matsubara & Hamada, 2006; Nagata, Guy, & Murakami, 2005; Nagumo et al., 2003). The examination on the medium strength steels showed a similar trend.

The results from Murakami and Matsunaga (2006) in Figure 6 indicated that fatigue life was reduced significantly with hydrogen charging. The fatigue test results from Wada, Ishigaki, Tanaka, Iwadate, and Ohnishi (2005) showed that hydrogen induced considerable reductions in cycles to failure as well, but the reduction tended to be less as the plastic strain range decreased. Meanwhile, Wada et al. (2006) found that the fatigue limit was not influenced by hydrogen.

The investigation on a tempered martensitic NiCrMo steel (Macadre et al., 2011) showed that with hydrogen charging, the decrease in fatigue life was significant, about 20% of that uncharged samples. However, the difference between fatigue limits of the uncharged and charged specimens was not obvious.

The low cycle fatigue (LCF) life of 2.25Cr1Mo (Han & Feng, 1995) was reduced remarkably, about 80%, by hydrogen compared with non-hydrogen charging. SEM analyses indicated that hydrogen atoms accelerated crack initiation of LCF from inclusions and transferred the

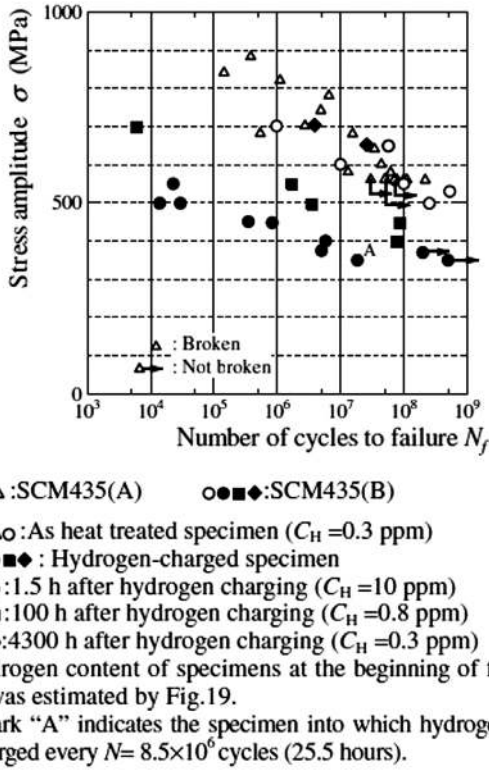

Figure 6 Fatigue test results from Murakami and Matsunaga. Reprinted from Murakami and Matsunaga (2006) with permission from Elsevier.

source of LCF crack from the surface of specimen to the inclusion, which resulted in the considerable decrease in LCF life. However, the original stress amplitudes for hydrogen-charged specimens were higher than that of uncharged specimens at the same strain amplitude, and the difference between them increased with increasing strain amplitude. They stated that this phenomenon was attributable to the drag effect of hydrogen on the moving dislocations (Abraham & Altstetter, 1995; Oriani & Josephic, 1980), which was relieved with increasing cyclic number, considering more and more hydrogen accumulated toward interfaces and microvoids that initiated from the secondary phase particles.

For medium-strength steels, fatigue life could be reduced by almost 80% in the presence of hydrogen, whereas the decrease in fatigue limit is not that significant, much <10%.

7.2 The threshold stress intensity factor range (ΔK_{th}) for crack growth

In the presence of hydrogen, ΔK_{th} could be changed compared with the value obtained in air. The results given by Andreikiv and Goliyan (1986) showed that hydrogen reduced ΔK_{th} for 35KhN3MFA rotor steel. However, ΔK_{th} does not always decrease due to hydrogen. Shih and Donald (1981) showed that hydrogen had little influence on the ΔK_{th} of a NiMoV rotor steel. Meanwhile, there are some factors such as the stress ratio (R), temperature, yield stress of the material, and test frequency, that can affect the hydrogen influence on ΔK_{th}.

Balitskii, Boichenko, Sosnin, and Shokov (1987) found that ΔK_{th} decreased in the presence of hydrogen and decreased even more at a lower loading frequency.

The influence of hydrogen on the ΔK_{th} depends on the yield stress of the material. Romaniv, Nikiforchin, and Kozak (1985, 1987) measured da/dN vs. ΔK of 40 Kh and 35khN3MFA steels after tempering at different temperatures. The results given by Romaniv et al. (1985) indicated that in vacuum and air, ΔK_{th} decreased with increasing yield strength. In the presence of hydrogen, a strong negative influence of hydrogen on ΔK_{th} occurred only for metals with low $\sigma_{0.2}$ values. At medium $\sigma_{0.2}$ values, there was an increase in the thresholds ΔK_{th} in hydrogen compared with that in air. No obvious influence of hydrogen on ΔK_{th} of high-strength steels ($\sigma_{0.2}$>1500 MPa) was observed compared with that in air.

The stress ratio applied during testing could also affect hydrogen influence on ΔK_{th}. With increasing stress ratio R, ΔK_{th} decreased for both air and hydrogen environments (Iacoviello & Di Cocco, 2007). The study of Denk, Lepik, and Ebi (1993) indicated that for the 3.5NiCrMoV rotor steel, for positive R, ΔK_{th} in hydrogen decreased with increasing R. This agreed with the results of Musuva and Radon (1979). However, it is worth noting that the R dependence of ΔK_{th} on hydrogen was not significant.

Temperature is also an influential factor. Denk et al. (1993) showed that in air, the value of ΔK_{th} decreased as the temperature increased from 20 C to 100 C. In hydrogen, the threshold values increased at elevated temperatures, passing through a maximum at 60 C.

In conclusion, the influence of hydrogen on the ΔK_{th} is dependent on many factors such as loading frequency, stress ratio, hydrogen concentration, and the material. Generally, at room temperature, ΔK_{th} would be lower than that obtained in air in the presence of hydrogen.

7.3 FCG rate

With a hydrogen content of 0.08–0.25 ppm, the maximum increase in FCG of SNCM439 steel could be about 9 times that of uncharged specimens (Macadre et al., 2011). The FCG rate of 2.25Cr1Mo with a martensitic microstructure was increased in the hydrogen environment (Hippsley, 1987). Tau et al. (1996) agreed that hydrogen accelerated the FCG rate, but they mentioned that the hydrogen-assisted FCG rate for the tempered martensites increased significantly with decreasing tempering temperature. That is, the degree of hydrogen influence on the FCG rate depends on other factors as well such as frequency, stress ratio, and so forth.

Generally, at a lower frequency, there would be more time for hydrogen diffusing into the crack tip, leading to a higher FCG rate (Murakami & Matsuoka, 2010). The investigation the FCG behavior of 2NiCrMoV (Smith & Stewart, 1979) showed that the FCG rates was dependent on test frequency. With decreasing frequency, the influence of hydrogen on the FCG rates became more significant. Some researchers (Macadre et al., 2011; Musuva & Radon, 1979; Romaniv et al., 1987) found the same trend. Figure 7 is an example graph illustrating the accelerated FCG rate at lower frequency in the presence of hydrogen.

The stress ratio is also an important factor for the hydrogen influence on the FCG rate. The cyclic stress intensity range, ΔK, is related to maximum applied stress intensity, K_{max} by the function (Nanninga, Slifka, Levy, & White, 2010):

$$\Delta K=(1\text{-}R)K_{max}. \tag{21}$$

As R increases, K_{max} increases at a given ΔK. The investigation by Musuva and Radon (1979) presented that a higher

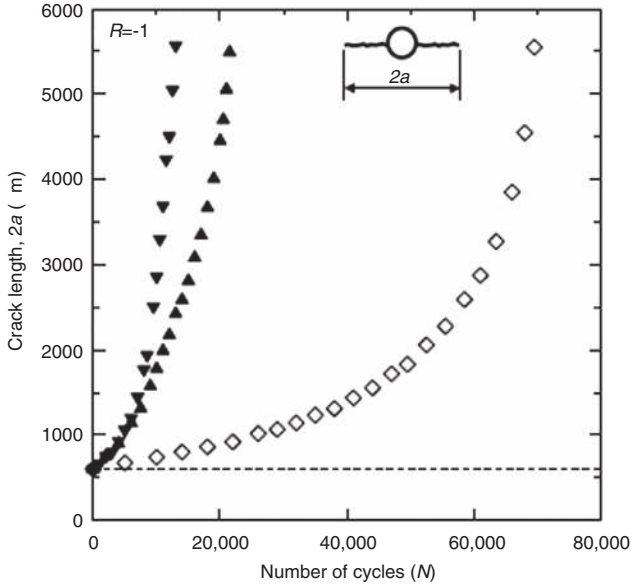

Symbol	Hydrogen charge	Frequency	C_H (mass ppm)
◇	Uncharged	20 Hz	≤ 0.01
▲	Gas	2 Hz	0.24→0.12
▼	Gas	0.2 Hz	0.25→0.08

Figure 7 Effect of frequency and environment on FCG rates of NiCrMo steel.
Reprinted from Macadre et al. (2011) with permission from Elsevier.

FCG rate can be caused by the increased positive stress ratio at a given value of ΔK, as demonstrated in Figure 8.

The hydrogen charging condition is also a factor. As mentioned previously, as the potential becomes more negative, more hydrogen is generated, leading to a more aggressive hydrogen condition (Atrens et al., 1980). Li, Wei, Zhang, and Tang (1993) found that for 12Mn-2V-B, the acceleration of the FCG rate by hydrogen was obvious and increased more at a more negative potential.

In most cases, for medium-strength steels, the FCG rate was accelerated by hydrogen. The significance of this acceleration could rely on many factors such as loading frequency and stress ratio. Generally, at room temperature, FCG could be accelerated by hydrogen up to two orders of magnitude.

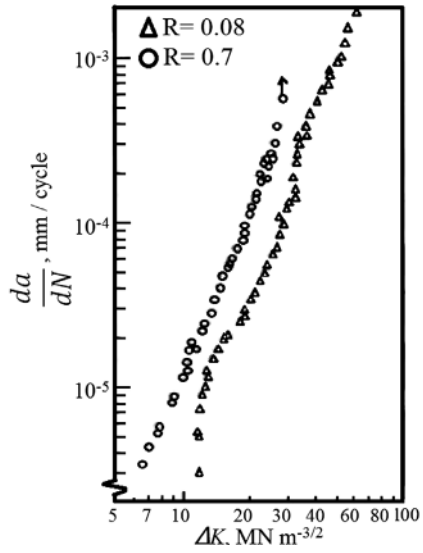

Figure 8 da/dN vs. ΔK at 0.25 Hz, B=12 mm (B is the thickness of the specimen).
Reprinted from Musuva and Radon (1979) with permission from Wiley.

7.4 Fatigue fracture features

In the presence of hydrogen, the fatigue fracture surface shows special features induced by hydrogen.

7.4.1 Hydrogen-inclusions interaction

As mentioned in the HEDE mechanism, the inclusion-matrix interface is attractive to hydrogen. The interaction between hydrogen and inclusions leads to different fracture features. Han and Feng (1995) found that the crack initiation for LCF occurred at the surface of uncharged 2.5Cr1Mo specimen, whereas for the hydrogen-charged specimen, the crack initiated as a microvoid at large inclusions including those containing Al and Mn. Han and Feng stated that the crack initiation at inclusions was because of the reduction in interface cohesive strength of the particle, and the acceleration of microvoid initiation at the inclusion, because of the high hydrogen concentration at the particle interface due to the high stress concentration and the high triaxial hydrostatic stress at the inclusion. Tsuchida et al. (2010) also found that fatigue cracks in uncharged S10C (low-carbon steel) specimens initiated at the surface and propagated into the specimen with a mechanism that produced striations on the fracture surface, whereas crack initiation after hydrogen charging was inside the specimen, resulting in a fish-eye mark on the fracture surface. Macadre et al. (2011) found fatigue cracks invariably initiated at large long clusters of Al_2O_3 inclusions for all smooth NiCrMo steel specimens, no matter uncharged or hydrogen-charged specimens, as shown in Figure 9. Fish-eye marks were frequently observed for cracks originating from inner defects such as single inclusions and small inclusion clusters (Li et al., 2008). Murakami, Nomoto, and Ueda (2000) stated that hydrogen trapped by nonmetallic inclusions was a crucial factor during fatigue and that careful attention

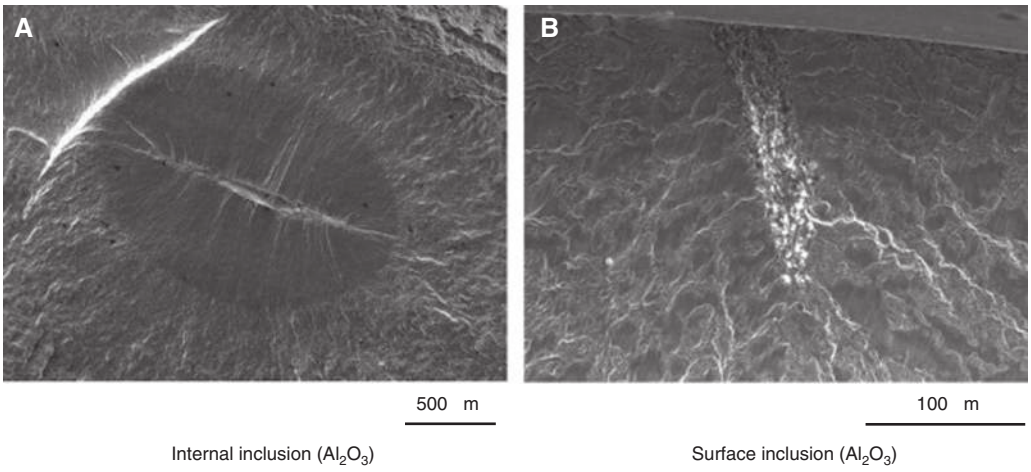

Figure 9 Fracture origins: (A) internal inclusions and (B) surface inclusion.
Reprinted from Macadre et al. (2011) with permission from Elsevier.

should be paid to inclusions when evaluating fatigue properties.

7.4.2 Other features induced by hydrogen

The observation of the fatigue features on stainless steels showed that with hydrogen charging, (i) discrete and localized slip bands were nucleated (Kanezaki et al., 2008; Murakami & Matsuoka, 2010; Uyama, Mine, Murakami, Nakashima, & Morishige, 2005; Uyama, Nakashima, Morishige, Mine, & Murakami, 2006), (ii) the fatigue crack was more linear and much thinner than that in the uncharged specimens (Kanezaki et al., 2008; Murakami & Matsuoka, 2010), (iii) the area fraction of striation and the striation height were reduced (Aoki, Kawamoto, Oda, Noguchi, & Higashida, 2005; Kanezaki et al., 2008), and (iv) the striation spacing was wider (Aoki et al., 2005); hydrogen accelerated the FCG rate. They (Aoki et al., 2005; Kanezaki et al., 2008; Murakami & Matsuoka, 2010; Uyama et al., 2005, 2006) stated that these changes were due to hydrogen-enhanced slip localization at the fatigue crack tip, which led to a decrease in the plastic zone size, which is an increasingly localized plastic deformation at the fatigue crack tip. These changes in fatigue features could be applicable to medium-strength steels.

Furthermore, intergranular fracture could be induced by hydrogen. Zima and Kozak (1986) showed that for 35KhN3MFA steel in medium-strength conditions, a considerable number of intergranular facets were observed. Compared with tests in vacuum or in air, the exceptional fractographic resolution of the striations was obtained in gaseous hydrogen. Zima and Kozak concluded that gaseous hydrogen promoted the occurrence of micromechanism of striation formation in the low- and medium-strength conditions. Takeda and McMahon (1981) observed two types of hydrogen-induced cracking (HIC): plasticity-related HIC (PRHIC) and intergranular HIC (IGHIC). They stated that PRHIC was strain controlled and intrinsic to steel deformed in hydrogen. It could not be avoided except by the exclusion of the hydrogen. IGHIC was considered as a stress-controlled mode and as the main mode in practice, especially in the early stage of cracking. IGHIC was attributed to impurity segregation at grain boundaries; thus, it could be decreased by steel purification and optimization of steel composition.

8 Microstructural effects on the resistance of steels to HE

For all steels, the yield strength is the critical factor determining the susceptibility to HE (Floreen, 1985). Steels possessing high yield strengths, especially for those higher than 1500 MPa, have poor resistance to HE. For lower yield strengths (<1000 MPa), the microstructure becomes an influential factor on HE resistance.

Hydrogen trapping in steels can affect and control their susceptibility to HE (Park, Koh, Jung, & Kim, 2008; Pressouyre, 1979, 1980, 1983; Pressouyre & Bernstein, 1978, 1981; Valentini & Salina, 1994). Pressouyre (1979) summarized potential traps for hydrogen in steels and classified those into three kinds: (i) attractive traps such as dislocations, crack tip, coherent and semicoherent grain boundaries and particles, and so forth; (ii) physical traps such as high-angle grain boundaries, voids, and incoherent particle-matrix interfaces (for example, incoherent

TiC, Fe_3C, and MnS) and so on; and (iii) mixed traps, i.e., combinations of the previous two types. He stated that attractive trapping was more reversible than physical trapping. Traps that really matter with the susceptibility to HE are reversible traps because irreversible traps function as sinks for hydrogen, making it hard for the hydrogen to jump out. It is believed that the best microstructure was to have no reversible traps but with a high, uniform density of fine, incoherent particles as irreversible traps (Pressouyre, 1979, 1980; Pressouyre & Bernstein, 1981). Thermal desorption spectroscopy (TDS) is a good method to investigate traps, including reversible and irreversible traps, in steels (Frappart et al., 2011; Hagi, 1997; Lee & Lee, 1986; Nagumo, Nakamura, & Takai, 2001; Pérez Escobar, Depover, Duprez, Verbeken, & Verhaege, 2012a; Wang, Akiyama, & Tsuzaki, 2005b; Wei, Hara, & Tsuzaki, 2004; Yagodzinskyy, Todoshchenko, Papula, & Hänninen, 2011). The TDS results would be helpful to improve the resistance to HE for steels.

The research by Park et al. (2008) showed that microstructures affected both hydrogen trapping and diffusion in steels and consequently influenced the resistance to HE. The hydrogen trapping efficiency was increased in the order of the degenerated pearlite, bainite (B), and acicular ferrite (AF), with AF being the most efficient. B was a more sensitive microstructure to HIC than was AF. As the microstructure changed from F/AF to F/B, the resistance to HIC decreased because the crack propagation was hindered by the high toughness of the AF.

Valentini and Salina (1994) stated the hydrogen influence on the behavior of steels was related to the trapping of hydrogen within the microstructure. Their results for 2.25Cr1Mo steel showed that although each the typical microstructure was martensite, because the different traps in the microstructure appeared at different temperatures, there was a big difference in the susceptibility to HE. The water quenched without tempering sample had the worst resistance to HE. The one tempered at 690 C presented the best resistance to HE. They explained that at this temperature, (i) there was a minimum number of reversible sites due to the dissolution of Mo_2C and (ii) there were irreversible sites due to M_7C_3 and $M_{23}C_6$ precipitates.

Luppo and Ovejero-Garcia (1991) stated that there was a direct relationship between HE susceptibility and the microstructure. Among the four microstructures they tested – equiaxial F and fine pearlite with some inclusions (normalized), lath martensite (quenched), tempered martensite at low temperature (QTL), and tempered martensite at high temperature (QTH, 773 K), the lath martensite had the lowest diffusion coefficient, highest quantity of desorbed hydrogen, and the worst resistance to HE. Meanwhile, QTH had the best resistance to HE, showing no loss in ductility and ductile fracture surface.

The investigation by Carneiro, Ratnapuli, and de Freitas Cunha Lins (2003) on the microstructure influence on HIC resistance of API pipeline indicated that the refined and homogeneous quenched and tempered B/martensite microstructures had the best performance with respect to HIC.

Even with the help of TDS, the effects of microstructure on the resistance to HE is still unclear. More work still needs to be done. Based on the data presented above, it is agreed that the tempered martensite microstructure usually is considered as having the best resistance to HE, and the untempered martensite the worst. Choosing a proper tempering condition for martensite microstructure steels is critical to get a good resistance to HE (Luppo & Ovejero-Garcia, 1991; Pressouyre, 1979; Valentini & Salina, 1994).

9 Concluding remarks

There are several aspects that needed to be addressed.

1. Although lots of effort had been put into the investigation of the hydrogen influence on steels, most of the research focused on high-strength steels, stainless steels, and pipeline steels. There are few studies focusing on the influence of hydrogen on medium-strength steels with a martensitic structure, or they were kept secret. Although some martensitic steels have already been safely in service for decades, it is beneficial to have a deeper understanding of the influence of hydrogen on these steels. That is needed for a more accurate estimation of the safe life of these components in service, and furthermore, to reduce damage due to hydrogen to the greatest possibility.
2. A systemized platform. The investigations concerning the hydrogen influence are numerous. However, it is still hard to estimate how significant the hydrogen influence is on an untested material because it is not easy to find a similar material that has been tested. Therefore, a systemized platform including all known information would be useful. The platform including all the test results to the present, such as the material composition, strength, microstructure, properties with and without hydrogen influence, would be very useful for estimating the behavior of a material in an environment with hydrogen. Thus, less effort would be needed to verify the preliminary assessment. This would be not only helpful for engineers when

choosing proper materials to use but this also good for accelerating the emergence of new materials. However, there are many difficulties, for example, some research studies are not public; test methods are not standardized. This is an ambitious proposal, requiring numerous human, material, and financial resources. It is difficult, but worthwhile.

3. Although some steels have mechanical strengths changed by a small amount in the presence of hydrogen, some steels exhibit significant loss of ductility due to hydrogen and may suffer catastrophic fast fracture. Such loss of ductility and propensity for fast fracture can have significant implications for service of the susceptible steels.
4. It is not clear why there can be significant differences in the influence of hydrogen on similar medium-strength steels, ranging from significant embrittlement to good resistance to hydrogen. This phenomenon merits further mechanistic research, particularly promising appears to be the study of hydrogen defect interactions using TDS (Frappart et al., 2011; Lee & Lee, 1986; Pérez Escobar et al., 2012a,b; Pérez Escobar, Duprez, Atrens, & Verbeken, 2013; Wei et al., 2004; Yagodzinskyy et al., 2011).
5. Modeling by computer. With the increasing science and technology, computer modeling is becoming more and more common and useful in the service. However, there are only a few models of interaction between hydrogen with steels (Fischer, Mori, & Svoboda, 2013; Legrand, Bouhattate, Feaugas, & Garmestani, 2012). Therefore, in the future, modeling could be an important direction for research.

Acknowledgments: This research is supported by an ARC linkage grant and by Alstom (Switzerland) Ltd.

Received May 22, 2013; accepted August 31, 2013; previously published online November 7, 2013

References

Abraham D, Altstetter C. The effect of hydrogen on the yield and flow stress of an austenitic stainless steel. Metall Mater Trans A 1995; 26: 2849–2858.

Addach H, Berçot P, Rezrazi M, Takadoum J. Study of the electrochemical permeation of hydrogen in iron. Corros Sci 2009; 51: 263–267.

Andreikiv AE, Goliyan OM. Subcritical fatigue crack growth in metals under the action of hydrogen. Mater Sci 1986; 21: 298–301.

Aoki Y, Kawamoto K, Oda Y, Noguchi H, Higashida K. Fatigue characteristics of a type 304 austenitic stainless steel in hydrogen gas environment. Int J Fracture 2005; 133: 277–288.

Arafin MA, Szpunar JA. Effect of bainitic microstructure on the susceptibility of pipeline steels to hydrogen induced cracking. Mater Sci Eng A 2011; 528: 4927–4940.

Araújo BA, Travassos GD, Silva AA, Vilar EO, Carrasco JP, de Araújo CJ. Experimental characterization of hydrogen embrittlement in API 5L X60 and API 5L X80 steels. Key Eng Mater 2011; 478: 34–39.

ASTM. Standard test method for determination of susceptibility of metals to embrittlement in hydrogen containing environments at high pressure, high temperature, or both. G142-98. West Conshohocken, PA: ASTM International, 2011.

ASTM. Standard test method for determination of the susceptibility of metallic materials to hydrogen gas embrittlement (HGE). F1459-06. West Conshohocken, PA: ASTM International, 2012a.

ASTM. Standard test method for measurement of hydrogen embrittlement threshold in steel by the incremental step loading technique. F1624-12. West Conshohocken, PA: ASTM International, 2012b.

Atrens A, Mezzanotte D, Fiore NF, Genshaw MA. Electrochemical studies of hydrogen diffusion and permeability in Ni. Corros Sci 1980; 20: 673–684.

Atrens A, Brosnan C, Ramamurthy S, Oehlert A, Smith I. Linearly increasing stress test (LIST) for SCC research. Meas Sci Technol 1993; 4: 1281–1292.

Bagotskaya IA. Effect of the solution composition on the diffusion rate of electrolytic hydrogen through metallic diaphragms. I. Diffusion of hydrogen through iron diaphragms. Zh Fiz Khim 1962; 36: 2667–2673.

Balitskii AI, Boichenko YA, Sosnin AV, Shokov NA. Cyclic crack resistance of rotor steel as a function of loading conditions. Metal Sci Heat Treat 1987; 29: 266–269.

Balitskii A, Krohmalny O, Ripey I. Hydrogen cooling of turbogenerators and the problem of rotor retaining ring materials degradation. Int J Hydrogen Energ 2000; 25: 167–171.

Barnoush A. Hydrogen embrittlement. Thesis. Saarbrücken: Saarland University, 2011.

Beachem C. A new model for hydrogen-assisted cracking (hydrogen "embrittlement"). Metall Mater Trans B 1972; 3: 441–455.

Beck W, Bockris J, Genshaw M, Subramanyan P. Diffusivity and solubility of hydrogen as a function of composition in Fe-Ni alloys. Metall Mater Trans B 1971; 2: 883–888.

Birnbaum HK. Mechanisms of hydrogen related fracture of metals. Report: USN 00014-83-K-0468. Urbana Champaign: University of Illinois, 1989.

Birnbaum HK, Sofronis P. Hydrogen-enhanced localized plasticity – a mechanism for hydrogen-related fracture. Mater Sci Eng A 1994; 176: 191–202.

Bockris JOM, Subramanyan PK. The equivalent pressure of molecular hydrogen in cavities within metals in terms of the overpotential developed during the evolution of hydrogen. Electrochim Acta 1971; 16: 2169–2179.

Bockris JOM, McBreen J, Nanis L. The hydrogen evolution kinetics and hydrogen entry into α-iron. J Electrochem Soc 1965; 112: 1025–1031.
Brass AM, Chêne J. Influence of tensile straining on the permeation of hydrogen in low alloy Cr-Mo steels. Corros Sci 2006; 48: 481–497.
Capelle J, Gilgert J, Pluvinage G. A fatigue initiation parameter for gas pipe steel submitted to hydrogen absorption. Int J Hydrogen Energ 2010; 35: 833–843.
Carneiro RA, Ratnapuli RC, de Freitas Cunha Lins V. The influence of chemical composition and microstructure of API linepipe steels on hydrogen induced cracking and sulfide stress corrosion cracking. Mater Sci Eng A 2003; 357: 104–110.
Caskey G Jr. Effect of hydrogen on work hardening of type 304L austenitic stainless steel. Scr Metall 1981; 15: 1183–1186.
Cracknell A, Petch NJ. Hydrogen and the yield point in steel. Acta Metall 1955; 3: 200.
Ćwiek J. Hydrogen degradation of high strength weldable steels. J Achiev Mater Manuf Eng 2007; 20: 223–226.
Ćwiek J. Prevention methods against hydrogen degradation of steel. Manuf Eng 2010; 43: 214–221.
Daynes HA. The process of diffusion through a rubber membrane. Proc R Soc Lond Ser A 1920; 97: 286–307.
Denk J, Lepik O, Ebi G. Effects of load ratio and gaseous environment on near threshold fatigue crack growth in a NiCrMoV rotor steel. In: Proc 5th Int Conf Fatigue Fatigue Thresholds, Quebec, Canada, 1993.
Devanathan MAV, Stachurski Z. The adsorption and diffusion of electrolytic hydrogen in palladium. P Roy Soc Lond A Mat 1962; 270: 90–102.
Dieter GE. Mechanical metallurgy. In: Mehl RF, Bever MB, editors. Metallurgy and metallurgical engineering series. New York: McGraw-Hill, 1961: 3–15.
Elboujdaini M, Revie RW. Metallurgical factors in stress corrosion cracking (SCC) and hydrogen-induced cracking (HIC). J Solid State Electrochem 2009; 13: 1091–1099.
Eliaz N, Shachar A, Tal B, Eliezer D. Characteristics of hydrogen embrittlement, stress corrosion cracking and tempered martensite embrittlement in high-strength steels. Eng Fail Anal 2002; 9: 167–184.
Fischer FD, Mori G, Svoboda J. Modelling the influence of trapping on hydrogen permeation in metals. Corros Sci 2013; 76: 382–389.
Floreen SF. Hydrogen cracking in specialty steels. In: Oriani RA, Hirth JP, Smialowski M, editors. Hydrogen degradation of ferrous alloys. Park Ridge, NJ: Noyes Publications, 1985: 799–821.
Frappart S, Oudriss A, Feaugas X, Creus J, Bouhattate J, Thébault F, Delattre L, Marchebois H. Hydrogen trapping in martensitic steel investigated using electrochemical permeation and thermal desorption spectroscopy. Scr Mater 2011; 65: 859–862.
Frappart S, Feaugas X, Creus J, Thebault F, Delattre L, Marchebois H. Hydrogen solubility, diffusivity and trapping in a tempered Fe-C-Cr martensitic steel under various mechanical stress states. Mater Sci Eng A 2012; 534: 384–393.
Fukuyama S, Yokoyawa K, Kudo K, Araki M. Fatigue properties of type 304 stainless steel in high pressure hydrogen at room temperature. Trans Jpn Inst Metal 1985; 26: 325.
Gamboa E, Atrens A. Environmental influence on the stress corrosion cracking of rock bolts. Eng Fail Anal 2003a; 10: 521–558.
Gamboa E, Atrens A. Stress corrosion cracking fracture mechanisms in rock bolts. J Mater Sci 2003b; 38: 3813–3829.
Gamboa E, Atrens A. Material influence on the stress corrosion cracking of rock bolts. Eng Fail Anal 2005; 12: 201–235.
Gangloff, RP. Hydrogen assisted cracking of high strength alloys, in Milne I, Ritchie RO, KB, editors. Comprehensive structural integrity. New York: Elsevier, 2003: 31–101.
Gangloff RP, Somerday BP, editors. Gaseous hydrogen embrittlement of materials in energy technologies: the problem, its characterisation and effects on particular alloy classes. Woodhead Publishing, 2012: 347–378.
Glowacka A, Swiatnicki WA. Effect of hydrogen charging on the microstructure evolution of duplex stainless steel. Mater Chem Phys 2003; 81: 496–499.
Glowacka A, Wozniak MJ, Swiatnicki WA. AFM study of austeno-ferritic stainless steel microstructure after cathodic hydrogen charging. J Alloy Compd 2005; 404–406: 595–598.
Grabke HJ, Riecke E. Absorption and diffusion of hydrogen in steels. Mater Tehnol 2000; 34: 331–342.
Hadam U, Zakroczymski T. Absorption of hydrogen in tensile strained iron and high-carbon steel studied by electrochemical permeation and desorption techniques. Int J Hydrogen Energ 2009; 34: 2449–2459.
Hagi H. Thermal evolution spectrum of hydrogen from low carbon steel charged by cathodic polarization. J Jpn Inst Metal 1997; 61: 274–281.
Han G, Feng D. Effects of hydrogen on behaviour of low cycle fatigue of 2.25Cr-1Mo steel. 25Cr-1Mo steel. J Mater Sci Technol 1995; 11: 358–362.
Hardie D, Xu J, Charles EA, Wei Y. Hydrogen embrittlement of stainless steel overlay materials for hydrogenators. Corros Sci 2004; 46: 3089–3100.
Hashimoto M, Latanision R. Experimental study of hydrogen transport during plastic deformation in iron. Metall Mater Trans A 1988a; 19: 2789–2798.
Hashimoto M, Latanision R. Theoretical study of hydrogen transport during plastic deformation in iron. Acta Metall 1988b; 36: 1837–1854.
Herms E, Olive JM, Puiggali M. Hydrogen embrittlement of 316L type stainless steel. Mater Sci Eng A 1999; 272: 279–283.
Hippsley CA. Hydrogen and temper embrittlement interactions in fatigue of 2.25Cr1Mo steel. 25Cr1Mo steel. Mater Sci Technol 1987; 3: 912–922.
Hirth J. Effects of hydrogen on the properties of iron and steel. Metall Mater Trans A 1980; 11: 861–890.
Holley CEJ, Worlton WJ, Zeigler RK. Compressibility factors and fugacity coefficients calculated from the Beattie-Bridgeman equation of state for hydrogen, nitrogen, oxygen, carbon dioxide, ammonia, methane, and helium. Report: LA-2271. Los Alamos, NM: Los Alamos Scientific Laboratory, 1958.
Iacoviello F, Di Cocco V. Sintered stainless steels: fatigue crack propagation resistance under hydrogen charging conditions. Corros Sci 2007; 49: 2099–2117.
Johnson WH. On some remarkable changes produced in iron and steel by the action of hydrogen and acids. Proc R Soc Lond 1874; 23: 168–179.
Kanezaki T, Narazaki C, Mine Y, Matsuoka S, Murakami Y. Effects of hydrogen on fatigue crack growth behavior of austenitic stainless steels. Int J Hydrogen Energ 2008; 33: 2604–2619.

Kishi A, Takano N. Effect of hydrogen cathodic charging on fatigue fracture of type 310S stainless steel. Int J Phys Conf Ser 2010; 240: 012050.

Kuromoto NK, Guimarães AS, Lepienski CM. Superficial and internal hydrogenation effects on the fatigue life of austenitic steels. Mater Sci Eng A 2004; 381: 216–222.

Labidi M, Habashi M, Tvrdy M, Galland J. Mechanisms of hydrogen embrittlement during low cycle-fatigue in metastable austenite. In: Rie K-T, Grünling HW, König G, Neumann P, Nowack H, Schwalbe K-H, Seeger T, editors. Low cycle fatigue and elasto-plastic behaviour of materials – 3. The Netherlands: Springer, 1992: 627–633.

Lasia A, Gregoire D. General model of electrochemical hydrogen absorption into metals. J Electrochem Soc 1995; 142: 3393–3399.

Lee J-Y, Lee SM. Hydrogen trapping phenomena in metals with B.C.C. and F.C.C. crystals structures by the desorption thermal analysis technique. Surf Coat Technol 1986; 28: 301–314.

Legrand E, Bouhattate J, Feaugas X, Garmestani H. Computational analysis of geometrical factors affecting experimental data extracted from hydrogen permeation tests: II – consequences of trapping and an oxide layer. Int J Hydrogen Energ 2012; 37: 13574–13582.

Li M-Q, Wei Z-W, Zhang F-S, Tang J-Q. The corrosion fatigue of medium strength structural steels. Corros Sci 1993; 34: 1403–1410.

Li D, Gangloff R, Scully J. Hydrogen trap states in ultrahigh-strength AERMET 100 steel. Metall Mater Trans A 2004; 35: 849–864.

Li YD, Yang ZG, Liu YB, Li SX, Li GY, Hui WJ, Weng YQ. The influence of hydrogen on very high cycle fatigue properties of high strength spring steel. Mater Sci Eng A 2008; 489: 373–379.

Lino M. Hydrogen-induced blister cracking of linepipe steel. In: Oriani RA, Hirth JP, Smialowski M, editors. Hydrogen degradation of ferrous alloys: Park Ridge, NJ: Noyes Publications, 1985: 737–762.

Liu Q, Irwanto B, Atrens A. The influence of hydrogen on 3.5NiCrMoV steel studied using the linearly increasing stress test. 5NiCrMoV steel studied using the linearly increasing stress test. Corros Sci 2013; 67: 193–203.

Louthan MR Jr, Caskey GR Jr, Donovan JA, Rawl DE Jr. Hydrogen embrittlement of metals. Mater Sci Eng 1972; 10: 357–368.

Lukito H, Szklarska-Smialowska Z. Susceptibility of medium-strength steels to hydrogen-induced cracking. Corros Sci 1997; 39: 2151–2169.

Luppo MI, Ovejero-Garcia J. The influence of microstructure on the trapping and diffusion of hydrogen in a low carbon steel. Corros Sci 1991; 32: 1125–1136.

Lynch SP. Environmentally assisted cracking: overview of evidence for an adsorption-induced localised-slip process. Acta Metall 1988; 36: 2639–2661.

Lynch SP. Comments on "A unified model of environment-assisted cracking". Scr Mater 2009; 61: 331–334.

Lynch S. Hydrogen embrittlement phenomena and mechanisms. Corros Rev 2012; 30: 105–123.

Macadre A, Yano H, Matsuoka S, Furtado J. The effect of hydrogen on the fatigue life of Ni-Cr-Mo steel envisaged for use as a storage cylinder for a 70 MPa hydrogen station. Int J Fatigue 2011; 33: 1608–1619.

Maier HJ, Popp W, Kaesche H. Effects of hydrogen on ductile fracture of a spheroidized low alloy steel. Mater Sci Eng A 1995; 191: 17–26.

Marchetti L, Herms E, Laghoutaris P, Chêne J. Hydrogen embrittlement susceptibility of tempered 9%Cr-1%Mo steel. Int J Hydrogen Energ 2011; 36: 15880–15887.

Matsubara Y, Hamada H. A novel method to evaluate the influence of hydrogen on fatigue properties of high strength steels. J ASTM Int 2006; 3: 1–14.

Matsui H, Kimura H, Moriya S. The effect of hydrogen on the mechanical properties of high purity iron I. Softening and hardening of high purity iron by hydrogen charging during tensile deformation. Mater Sci Eng 1979; 40: 207–216.

McBreen J, Nonis L, Beck W. A method for determination of the permeation rate of hydrogen through metal membranes. J Electrochem Soc 1966; 113: 1218–1222.

Moon AP, Balasubramaniam R, Panda B. Hydrogen embrittlement of microalloyed rail steels. Mater Sci Eng A 2010; 527: 3259–3263.

Moro I, Briottet L, Lemoine P, Andrieu E, Blanc C, Odemer G. Hydrogen embrittlement susceptibility of a high strength steel X80. Mater Sci Eng A 2010; 527: 7252–7260.

Mukhopadhyay N, Sridhar G, Parida N, Tarafder S, Ranganath V. Hydrogen embrittlement failure of hot dip galvanised high tensile wires. Eng Fail Anal 1999; 6: 253–265.

Murakami Y, Matsunaga H. The effect of hydrogen on fatigue properties of steels used for fuel cell system. Int J Fatigue 2006; 28: 1509–1520.

Murakami Y, Matsuoka S. Effect of hydrogen on fatigue crack growth of metals. Eng Fract Mech 2010; 77: 1926–1940.

Murakami Y, Nomoto T, Ueda T. On the mechanism of fatigue failure in the superlong life regime (N>107 cycles). Part 1: influence of hydrogen trapped by inclusions. Fatigue Fract Eng Mater Struct 2000; 23: 893–902.

Musuva J, Radon J. The effect of stress ratio and frequency on fatigue crack growth. Fatigue Fract Eng Mater Struct 1979; 1: 457–470.

Nagata J, Guy N, Murakami Y. Effect of hydrogen charge on fatigue strength of martensitic stainless steel. J Soc Mater Sci, Japan 2005; 54: 1217–1224.

Nagumo M. Hydrogen related failure of steels – a new aspect. Mater Sci Technol 2004; 20: 940–950.

Nagumo M, Nakamura M, Takai K. Hydrogen thermal desorption relevant to delayed-fracture susceptibility of high-strength steels. Metall Mater Trans A 2001; 32: 339–347.

Nagumo M, Shimura H, Chaya T, Hayashi H, Ochiai I. Fatigue damage and its interaction with hydrogen in martensitic steels. Mater Sci Eng A 2003; 348: 192–200.

Nanninga N, Slifka A, Levy Y, White C. A review of fatigue crack growth for pipeline steels exposed to hydrogen. J Res Natl Inst Stan 2010; 115: 437–452.

Nanninga NE, Levy YS, Drexler ES, Condon RT, Stevenson AE, Slifka AJ. Comparison of hydrogen embrittlement in three pipeline steels in high pressure gaseous hydrogen environments. Corros Sci 2012; 59: 1–9.

Nelson HG, editors. Hydrogen embrittlement. In: Briant CL, Banerji SK, editors. Treatise on materials science and technology. New York: Academic Press, 1983: 275–359.

Oehlert A, Atrens A. The initiation and propagation of stress corrosion cracking in AISI 4340 and 3.5 Ni-Cr-Mo-V rotor steel in constant load tests. 5 Ni-Cr-Mo-V rotor steel in constant load tests. Corros Sci 1996; 38: 1159–1169.

Oguri K, Takaki S, Kimura H. Hydrogen-induced softening and hardening in high purity Fe-C alloys. Mater Sci Eng 1982; 53: 223–232.

Oriani RA, Josephic PH. Effects of hydrogen on the plastic properties of medium-Carbon steels. Metall Trans A 1980; 11: 1809–1820.

Oriani RA, Hirth JP, Smialowski M, editors. Hydrogen degradation of ferrous alloys. Park Ridge, NJ: Noyes Publications, 1985.

Pan C, Su YJ, Chu WY, Li ZB, Liang DT, Qiao LJ. Hydrogen embrittlement of weld metal of austenitic stainless steels. Corros Sci 2002; 44: 1983–1993.

Panagopoulos CN, El-Amoush AS, Georgarakis KG. The effect of hydrogen charging on the mechanical behaviour of [alpha]-brass. J Alloy Compd 2005; 392: 159–164.

Park GT, Koh SU, Jung HG, Kim KY. Effect of microstructure on the hydrogen trapping efficiency and hydrogen induced cracking of linepipe steel. Corros Sci 2008; 50: 1865–1871.

Pasco RW. Entry of hydrogen from the gas phase. In: RA Oriani, JP Hirth, M Smialowski, editors. Hydrogen degradation of ferrous alloys. Park Ridge, NJ: Noyes Publications, 1985.

Pérez Escobar D, Depover T, Duprez L, Verbeken K, Verhaege M. Combined thermal desorption spectroscopy, differential scanning calorimetry, scanning electron microscopy and X-ray diffraction study of hydrogen trapping in cold deformed TRIP steel. Acta Mater 2012a; 60: 2593–2605.

Pérez Escobar D, Depover T, Wallaert E, Duprez L, Verhaege M, Verbeken K. Thermal desorption spectroscopy study of the interaction between hydrogen and different microstructural constituents in lab cast Fe-C alloys. Corros Sci 2012b; 65: 199–208.

Pérez Escobar D, Duprez L, Atrens A, Verbeken K. Influence of experimental parameters on thermal desorption spectroscopy measurements during evaluation of hydrogen trapping. J Nucl Mater 2013.

Perng TP, Wu JK. A brief review note on mechanisms of hydrogen entry into metals. Mater Lett 2003; 57: 3437–3438.

Perujo A, Serra E, Alberici S, Tominetti S, Camposilvan J. Hydrogen in the martensitic DIN 1.4914: a review. J Alloy Compd 1997; 253–254: 152–155.

Petch NJ, Stables P. Delayed fracture of metals under static load. Nature 1952; 169: 842–843.

Popov KV, Nechai EP. Theory of hydrogen embrittlement of metals. Phys-Chem Mech Mater 1967; 3: 459–473.

Pressouyre GM. A classification of hydrogen traps in steel. Metall Trans A 1979; 10: 1571–1573.

Pressouyre GM. Trap theory of Hydrogen embrittlement. Acta Metall 1980; 28: 895–911.

Pressouyre G. Hydrogen traps, repellers, and obstacles in steel; Consequences on hydrogen diffusion, solubility, and embrittlement. Metall Mater Trans A 1983; 14: 2189–2193.

Pressouyre G, Bernstein I. A quantitative analysis of hydrogen trapping. Metall Mater Trans A 1978; 9: 1571–1580.

Pressouyre GM, Bernstein IM. An example of the effect of hydrogen trapping on hydrogen embrittlement. Metall Trans A 1981; 12: 835–844.

Raja VS, Shoji T, editors. Stress corrosion cracking: theory and practice. Cambridge: Woodhead Publishing, 2011: 90–126.

Ramamurthy S, Atrens A. The influence of applied stress rate on the stress corrosion cracking of 4340 and 3.5NiCrMoV steels in distilled water at 30 C. Corros Sci 2010; 52: 1042–1051.

Ramamurthy S, Atrens A. Stress corrosion cracking of high-strength steels. Corros Rev 2013; 31: 1–31.

Ramamurthy S, Lau WML, Atrens A. Influence of the applied stress rate on the stress corrosion cracking of 4340 and 3.5NiCrMoV steels under conditions of cathodic hydrogen charging. Corros Sci 2011; 53: 2419–2429.

Romaniv ON, Nikiforchin GN, Kozak LY. Structural sensitivity of the cyclic crack resistance of rotor steel in gaseous hydrogen. Mater Sci 1985; 20: 424–429.

Romaniv O, Nikiforchin G, Kozak LY. Cyclic crack resistance of constructional steels in gaseous hydrogen. Mater Sci 1987; 22: 439–450.

Shih TT, Donald JK. Threshold and low-rate fatigue crack growth of a NiMoV rotor steel. J Eng Mater Technol 1981; 103: 104–111.

Siddiqui RA, Abdullah HA. Hydrogen embrittlement in 0.31% carbon steel used for petrochemical applications. J Mater Process Tech 2005; 170: 430–435.

Smith P, Stewart A. Effect of aqueous and hydrogen environments on fatigue crack growth in 2Ni-Cr-Mo-V rotor steel. Metal Sci 1979; 13: 429–435.

Sojka J, Vodárek V, Schindler I, Ly C, Jérôme M, Váňová P, Ruscassier N, Wenglorzová A. Effect of hydrogen on the properties and fracture characteristics of TRIP 800 steels. Corros Sci 2011; 53: 2575–2581.

Sudarshan TS, Louthan MR Jr, McNitt RP. Hydrogen induced suppression of yield point in A-106 steel. Scr Metall 1978; 12: 799–803.

Takeda Y, McMahon CJ. Strain controlled vs stress controlled hydrogen induced fracture in a quenched and tempered steel. Metall Trans A 1981; 12: 1255–1266.

Tau L, Chan SLI, Shin CS. Hydrogen enhanced fatigue crack propagation of bainitic and tempered martensitic steels. Corros Sci 1996; 38: 2049–2060.

Thomson R. Brittle fracture in a ductile material with application to hydrogen embrittlement. J Mater Sci 1978; 13: 128–142.

Toribio J. Hydrogen-plasticity interactions in pearlitic steel: a fractographic and numerical study. Mater Sci Eng A 1996; 219: 180–191.

Toribio J, Lancha A, Elices M. Characteristics of the new tearing topography surface. Scr Metall Mater 1991a; 25: 2239–2244.

Toribio J, Lancha AM, Elices M. Hydrogen embrittlement of pearlitic steels: phenomenological study on notched and pre-cracked specimens. Corrosion 1991b; 47: 781–791.

Torres-Islas A, Salinas-Bravo VM, Albarran JL, Gonzalez-Rodriguez JG. Effect of hydrogen on the mechanical properties of X-70 pipeline steel in diluted NaHCO3 solutions at different heat treatments. Int J Hydrogen Energ 2005; 30: 1317–1322.

Troiano AR. The role of hydrogen and other interstitials in the mechanical behaviour of metals. Trans ASM 1960; 52: 54–80.

Tsuchida Y, Watanabe T, Kato T, Seto T. Effect of hydrogen absorption on strain-induced low-cycle fatigue of low carbon steel. Procedia Eng 2010; 2: 555–561.

Uyama H, Mine Y, Murakami Y, Nakashima M, Morishige K. Effects of hydrogen charge on cyclic stress-strain properties and fatigue behavior of carbon steels. J Soc Mater Sci Jpn 2005; 54: 1225–1230.

Uyama H, Nakashima M, Morishige K, Mine Y, Murakami Y. Effects of hydrogen charge on microscopic fatigue behaviour of annealed carbon steels. Fatigue Fract Eng Mater Struct 2006; 29: 1066–1074.

Valentini R, Salina A. Influence of microstructure on hydrogen embrittlement behaviour of 2·25Cr-1 Mo steel. Mater Sci Technol 1994; 10: 908–914.
Villalba E, Atrens A. An evaluation of steels subjected to rock bolt SCC conditions. Eng Fail Anal 2007; 14: 1351–1393.
Villalba E, Atrens A. Metallurgical aspects of rock bolt stress corrosion cracking. Mater Sci Eng A 2008a; 491: 8–18.
Villalba E, Atrens A. SCC of commercial steels exposed to high hydrogen fugacity. Eng Fail Anal 2008b; 15: 617–641.
Villalba E, Atrens A. Hydrogen embrittlement and rock bolt stress corrosion cracking. Eng Fail Anal 2009; 16: 164–175.
Wada Y, Ishigaki R, Tanaka Y, Iwadate T, Ohnishi K. Evaluation of metal materials for hydrogen fuel stations. In: Proc Int Conf Hydrogen Safety, Pisa, 2005: 8–10.
Wang J-S. On the diffusion of gases through metals. Math Proc Cambridge 1936; 32: 657–662.
Wang R. Effects of hydrogen on the fracture toughness of a X70 pipeline steel. Corros Sci 2009; 51: 2803–2810.
Wang M, Akiyama E, Tsuzaki K. Effect of hydrogen and stress concentration on the notch tensile strength of AISI 4135 steel. Mater Sci Eng A 2005a; 398: 37–46.
Wang M, Akiyama E, Tsuzaki K. Hydrogen degradation of a boron-bearing steel with 1050 and 1300MPa strength levels. Scr Mater 2005b; 52: 403–408.
Wang M, Akiyama E, Tsuzaki K. Effect of hydrogen on the fracture behavior of high strength steel during slow strain rate test. Corros Sci 2007; 49: 4081–4097.
Wei F, Hara T, Tsuzaki K. Precise determination of the activation energy for desorption of hydrogen in two Ti-added steels by a single thermal-desorption spectrum. Metall Mater Trans B 2004; 35: 587–597.
West AJ, Louthan MR. Hydrogen effects on the tensile properties of 21-6-9 stainless steel. Metall Mater Trans A 1982; 13: 2049–2058.
Yagodzinskyy Y, Todoshchenko O, Papula S, Hänninen H. Hydrogen solubility and diffusion in austenitic stainless steels studied with thermal desorption spectroscopy. Steel Res Int 2011; 82: 20–25.
Yan M, Weng Y. Study on hydrogen absorption of pipeline steel under cathodic charging. Corros Sci 2006; 48: 432–444.
Zakroczymski T. Entry of hydrogen into iron alloys from the liquid phase. In: Oriani RA, Hirth JP, Smialowski M, editors. Hydrogen degradation of ferrous alloys. Park Ridge, NJ: Noyes Publications, 1985: 215–224.
Zakroczymski T, Glowacka A, Swiatnicki W. Effect of hydrogen concentration on the embrittlement of a duplex stainless steel. Corros Sci 2005; 47: 1403–1414.
Zapffe C, Sims C. Hydrogen embrittlement, internal stress and defects in steel. Trans AIME 1941; 145: 225–271.
Zhang TY, Zheng YP. Effects of absorption and desorption on hydrogen permeation – I. Theoretical modeling and room temperature verification. Acta Mater 1998; 46: 5023–5033.
Zhang TY, Zheng YP, Wu QY. On the boundary conditions of electrochemical hydrogen permeation through iron. J Electrochem Soc 1999; 146: 1741–1750.
Zima YV, Kozak LY. Fractographic aspects of the cyclic crack resistance of 35KhN3MFA steel in vacuum, air, and hydrogen. Mater Sci 1986; 22: 268–275.

Qian Liu is a senior PhD student at the University of Queensland. She received her Bachelor's and Master's degrees in Engineering from the University of Science and Technology, Beijing, China. She is currently working on the influence of hydrogen on the metallic components for clean energy. She spent 5 months in Switzerland in 2012 for her PhD research.

Andrej Atrens is Professor of Materials at the University of Queensland, where he has been since 1984. He has an international academic reputation, as evidenced by invitations for keynote papers at international conferences (17 papers since 2001), invitations as guest scientist/visiting professor at leading international laboratories (in Belgium, Switzerland, Germany, France, and Sweden; 22 months since 2003), a high ISI H-index of 39 (Web of Science), a number of citations (5570 citations, Web of Science), eight journal papers with more than 100 citations, six journal papers with more than 200 citations, and an excellent publication record in top international journals with more than 200 refereed journal publications. His areas of research are SCC, corrosion of magnesium, corrosion mechanisms, atmospheric corrosion, and pagination of copper.